Journal of Zhejiang University-SCIENCE A (Applied Physics & Engineering)
ISSN 1673-565X (Print); ISSN 1862-1775 (Online)
www.zju.edu.cn/jzus; www.springerlink.com
E-mail: jzus@zju.edu.cn

An experimental investigation of properties of polyethylene reinforced with Al powders

Victoria CHIFOR[1], Zafer TEKINER[‡2], Mehmet TURKER[2], Radu ORBAN[1]

([1]*Department of Materials Science and Technology, Faculty of Materials Science and Engineering, Technical University of Cluj-Napoca, Cluj-Napoca 400641, Romania*)

([2]*Mechanical/Metallurgy Education Department, Faculty of Technical Education, Gazi University, Ankara 06500, Turkey*)

E-mail: chifor_victoria@yahoo.com; ztekiner@gazi.edu.tr; mturker@gazi.edu.tr; Radu.Orban@stm.utcluj.ro

Received June 16, 2010; Revision accepted Oct. 22, 2010; Crosschecked July 19, 2011

Abstract: Mechanical and physical properties, such as tensile strength, elongation at break, modulus of elasticity, Shore D hardness, melt flow rate (MFR), and electrical and thermal conductivities of composites with high density polyethylene matrix reinforced with Al powders were investigated experimentally. Measurements of the mechanical and physical properties were performed up to a reinforcing component concentration of 30% volume Al powder and compared with mathematical models from the literature. The obtained results have shown that experimental data were in good agreement with theoretical data. The ultimate tensile strength (UTS) and elongation at break decreased with increasing Al powder content, which was attributed to the introduction of discontinuities in the polymer structure, and modulus of elasticity increased with increasing Al content. The composite preparation conditions allowed the formation of a random distribution of metallic particles in the polymer matrix volume for system high density polyethylene-Al (HDPE-Al). There was a cluster formation of Al particles at higher Al contents in the polymer matrix. Electrical and thermal conductivity values of HDPE-Al composites were higher than pure HDPE values.

Key words: Polymer composite, Mechanical properties, Melt flow rate (MFR), Thermal conductivity, Electrical conductivity
doi:10.1631/jzus.A1000286 **Document code:** A **CLC number:** TB32

1 Introduction

Metal powders play an important role in the production of polymeric materials. In addition to cost saving (Bader, 2002; Park *et al.*, 2009), other value-added properties are gained through the use of fillers. Metal powders can improve optical and mechanical (Han and Jang, 1999), thermal (Progelhof *et al.*, 1976), and electrical (Lux, 1993) properties of polymer materials. Polymers can be modified with metallic powders for more specific uses such as anti-fouling compounds, corrosion-resistant paints, and maintenance products such as cold-poured steel and tooling. Metal filled polymer composites are often used as heating elements, temperature-dependence resistors and sensors, self-limiting electrical heaters and switching devices, and antistatic materials for electromagnetic interference shielding of electronic devices, etc. They are much cheaper than metals. Some of these materials are multifunctional, environmentally friendly, offer better corrosion resistance than metals and, in most cases, require only one-step processing, compared to the great number of steps involved in metal processing.

The conductivity of polymer composites that contain dispersed conductive fillers depends on many factors such as the size and the shape of the filler particles, their spatial distribution within a polymer matrix, and the interactions between the filler surface and the polymer matrix (Gavarri *et al.*, 1999; Kovacs *et al.*, 2007). Additionally, their electrical and thermal conductivity levels can be designed in order to satisfy the various requirements of the end users. The

‡ Corresponding author

physical and mechanical properties: type, characteristics, and proportion of polymeric matrix/reinforcing component correlation must be known to determine the usefulness and application of these materials. It is therefore important, from both the scientific and practical viewpoints, to understand the effects of powder addition as a reinforcing component on the properties of a polymer matrix.

In this work, the effect of the volume fraction of filler metal powder on the mechanical properties and conductivity behaviour of polymer was researched.

2 Materials and methods

2.1 Materials

High density polyethylene (HDPE) produced by Petkim (Turkey) was used as the matrix component. HDPE has the density of 0.95 g/cm^3, melting start point of 110 °C, and molecular weight of 10^5 g/mol. Aluminium powder (99% purity) of irregular particle shape, with the particle size distribution of 200 μm produced by Ecka Granules were used as the reinforcing material.

2.2 Composite preparation

The composites were prepared by mixing the polymer and various amounts of metallic powders in a Szegvari type attritor. Samples were measured according to the required volume and then mixed at room temperature at a speed of 250 r/min in argon atmosphere. HDPE-Al mixtures were extruded to prepare homogenous feedstock. The samples were injected in an HM 300 Super injection moulding machine at a pressure of 80 MPa and temperature of 190–235 °C depending on the reinforcing amount and were allowed to cool at room temperature. Injection mould cavity was produced according to ASTM D638-10 (2010). Standard sample dimensions were given in Table 1 and Fig. 1.

2.3 Scanning electron microscopy (SEM)

The SEM micrographs were taken at different magnifications of 350X and 500X, using JEOL JSM-6060 LV SEM device (Japan).

2.4 Rheological measurements

Rheological properties of the polymer matrix composite were investigated using a Llyod trade mark MF-I 10 model melt flow indexer with a capillary length l=8 mm, a diameter of capillary D_c=2.095 mm, a diameter of barrel D=9.47 mm, and the pressure P=298.2 Pa. Melt flow rate (MFR) and viscosity values were obtained according to the standard test method for MFRs of thermoplastics by extrusion plastometer (ASTM D1238-10, 2010). Measurements were carried out on a sample of 2160 g at 190 °C. The final melt flow rate and viscosity results were evaluated from the average of three different measurements.

Table 1 Test specimen type 5A (ASTM D638-10, 2010)

Parameter	Standard dimension (mm)	Sample dimension (mm)
L_2	≥75	75
b_2	12.5±1	12.5
L_1	25±1	25
b_1	4±0.1	4
r_1	8±0.5	8
r_2	12.5±1	12.5
L	50+2	50
L_0	20+0.5	20
h	≥2	3

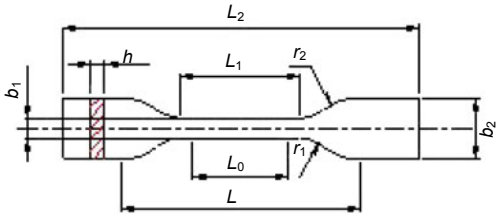

Fig. 1 Sample dimension

L: distance between grips; L_0: gage length; L_1: length of narrow section; L_2: overall length; r_1: radius of fillet; r_2: outer radius; b_1: narrow width; b_2: overall width; h: sample thickness

2.5 Mechanical testing

The mechanical properties were measured at room temperature according to ASTM D638-10 (2010), using a Shimadzu Autograph AG-IS provided with control system, acquisition, and computer data processing. The samples were stretched at the speed of 50 mm/min under a cell load of 2500 N. The mechanical properties were obtained using the average value of three experimental test samples values. Fracture surface of the specimens was examined with an electron scanning electron microscope (Jeol, Japan).

Shore D hardness was obtained according to the standard test method for rubber property-durometer hardness (ASTM D2240-05, 2010) and was determined using GS-720G type device.

2.6 Electrical conductivity

A measure of the electrical resistance between opposite faces of a unit cube of material, gives volume resistively through an insulating body. The standard test methods for DC resistance or conductance of insulating materials (ASTM D257-07, 2007) measure resistance in Ω between electrodes mounted on opposite specimen faces (Fig. 2). This resistance is multiplied by the electrode's area and then divided by the sample thickness, to give the volume resistivity in Ω·cm. Finally, the volume resistivity is converted in electrical conductivity measured in S/m.

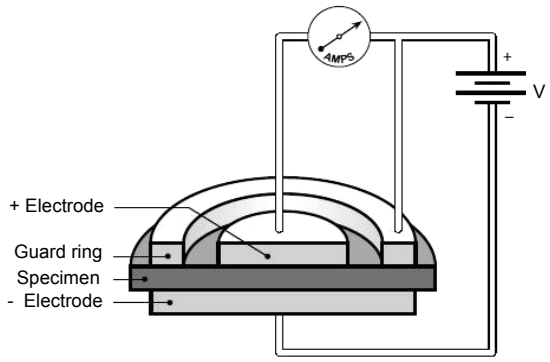

Fig. 2 Cross-sectional schematic of a typical volume-resistivity test apparatus

2.7 Thermal conductivity

The standard test for thermal transmission properties (ASTM C177-04, 2004) measures the steady-state heat flux through a flat-slab specimen, using a guarded hot-plate apparatus. In the test, a hot isothermal surface is placed between two specimens, with two cold plates placed on the specimens' outer sides (Fig. 3). These three isothermal units help to create a measurable, steady-state heat flux unidirectional through the specimens. Sensors measure heat transfer from the centre hot plate through the specimens to the cold plates.

3 Results and discussion

The morphological analyses of Al powder was carried out by JEOL JSM-6060 LV SEM device using the tension of 20 kV, and an electronic spot diameter of 20 μm in vacuum atmosphere (Fig. 4).

Fig. 4 shows the overall morphological appearance of Al powder particles with a particle analysis

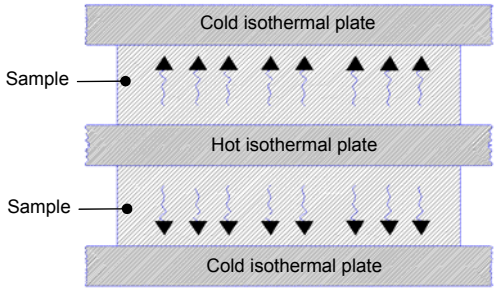

Fig. 3 Simplified schematic describing the test quantifying thermal transmission

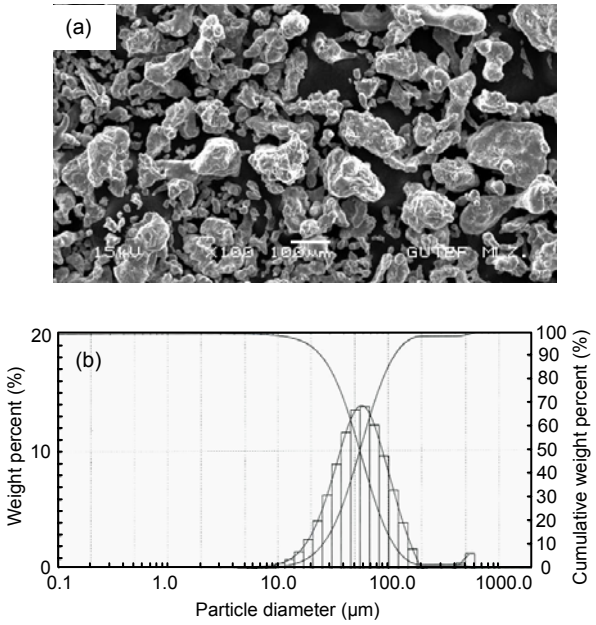

Fig. 4 SEM micrographs of Al powder particles (a) and the size analysis result (b)

result. As shown in the micrograph, the shapes of particles are irregular which are typically water atomised powders. The mean particle size of the particles is 55.66 μm. The mechanical and physical properties of HDPE and Al powder are given Table 2.

Shear stress can be obtained using the following equation as given in the standard test method for determination of properties of polymeric materials by means of a capillary rheometer (ASTM D3835-08, 2008):

$$\tau_a = \frac{(p - P_c)D}{4L_d} = \frac{(F - F_c)D}{4L_d A_B}, \quad (1)$$

Table 2 Mechanical and physical properties of HDPE and Al powder

Material	Density (g/cm³)	Viscosity at 190 °C (Pa·s)	MFR (g/10 min)	SR (s^{-1})	Hardness
HDPE	0.966–0.970	320	4.4–6.5	2700	64*
Al	2.702	–	–	–	95**
Material	TS (MPa)	EB (%)	ER (Ω·cm)	TC (W/(m·K))	EM (MPa)
HDPE	22	750	9×10^{-14}	0.386	200
Al	241	12	270×10^{-8}	167	6.8×10^{4}

* Shore D hardness; ** Brinell hardness; MFR: melt flow rate; SR: shear rate; TS: tensile strength; EB: elongation at break; ER: electrical resistivity; TC: thermal conductivity; EM: elastic modulus

where τ_a is the apparent shear stress, p is the melt pressure, P_c is the initial pressure of plunger force, D is the die diameter, L_d is the die length, F is the force applied on plunger, F_c is the intercept force, and A_B is the cross-sectional area of the barrel. Melt flow indexer measure the plunger force. This force drops inside of the barrel. In order to eliminate the pressure dropping effect, a Bagley correction was performed.

The Wiesenberger Rabinowitsch shear rate (ASTM D3835-08, 2008) correction accounts for the fact that the true shear rate is often larger than the apparent shear rate for non-Newtonian materials. The true shear rate can be calculated using the following equation:

$$\gamma = \frac{(3n+1)}{4n}\gamma_a, \tag{2}$$

where γ is the true shear rate, and γ_a is the apparent shear rate. n is the tangent slope of the log true shear stress versus log apparent shear rate curve with the apparent shear rate being corrected, which could be calculated from the linear line in Fig. 5.

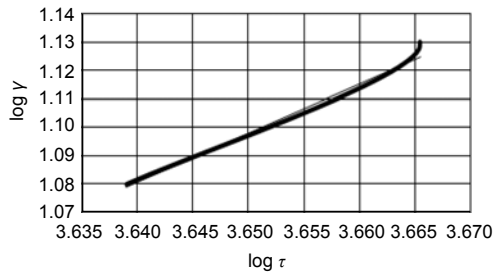

Fig. 5 Shear rate against shear stress at 190 °C

Perform calculations as follows:

$$\tau = \frac{FR}{2\pi R_p^2 L_c}, \tag{3}$$

$$\gamma = \frac{2.4MVR}{\pi R^3}, \tag{4}$$

$$\eta = \frac{\rho\pi r^4}{8L_c Q} = \frac{Fr^4 t}{8R^2 L_c V}, \tag{5}$$

where F is the force on ram (N), R is the radius of barrel (m), L_c is the length of capillary (m), V is the volume extruded (m^3), r is the radius of capillary (m), Q is the flow rate (m^3/s), t is the extrusion time (s), and τ is the true shear stress.

Coefficient n was calculated from the slopes of MFR against shear rate curve as 0.7649 (Fig. 5).

MFR was measured for every rate (5%–30%) of reinforcing elements within the matrix, and shear rate, shear stress, and viscosity were calculated according to the obtained values. Then Figs. 5–8 were plotted according to those values.

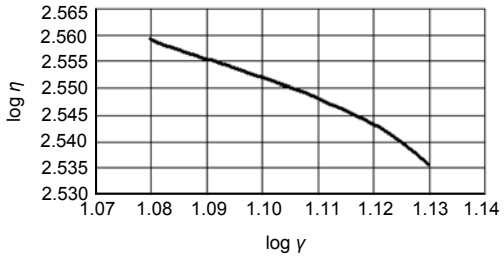

Fig. 6 Viscosity against shear rate at 190 °C

An increase in the amount of reinforcing elements in the composite resulted in an increase in the density of the polymer matrix composite that increases the amount of reinforcing elements in the composite. This density effect caused a decrease in the volumetric MFR (cm^3/10 min), whereas it results in an increase in mass MFR (g/10 min) of the polymer matrix composite. So Eq. (6) has been generated depending on the density (Fig. 7):

$$\mathrm{MFR_c} = 0.96\mathrm{MFR_m^{1.12}}\varphi D_f^{0.016}((1-\varphi)D_m)^{0.56}, \tag{6}$$

where $\mathrm{MFR_c}$ and $\mathrm{MFR_m}$ are the melt flow rates of the composite and the matrix, respectively, D_f and D_m are

the densities of the filler and the matrix, and φ is the packing factor. There is no experimental study on the sample containing more than one metallic powders.

It has been established, as an original contribution that the equations obtained by regression analyses to predict MFR.

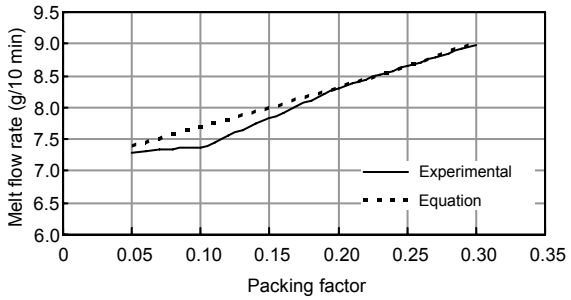

Fig. 7 MFR of HDPE-Al composites

The viscosity of the polymer matrix composite increased the packing factor reached 0.30 (Fig. 8). The rheological behaviour of a plastic-metal powder composite was a combination of non-Newtonian and Newtonian flow behaviours. At lower shear rates, the plastic-Al powder composite was non-Newtonian, but as the shear rate increased, the mixture composite tended to exhibit a Newtonian behaviour due to the fact that increasing shear rates cause the polymer molecules and Al particles to untangle from each other and align themselves in the flowing direction.

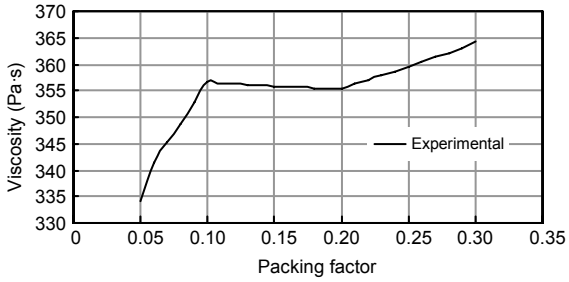

Fig. 8 Viscosity of HDPE-Al composites

SEM microscopy was used to investigate the distribution of metallic particles in the polymer matrix. The structure of composites, obtained by SEM microscopy at 10% (v/v) and 30% (v/v) Al is shown in Fig. 9. Al powder particle distribution was not uniform in the matrix that contained both low rate (10%, v/v) (Fig. 9b) and high rate (30%, v/v) (Fig. 9c) of Al particles, leading to the formation of a particle network in the whole material, which contributed to the improvement of Shore D hardness, especially in 30% (v/v) Al HDPE matrix (Fig. 10). Examined SEM pictures, particle fillers, type, concentration, size, shape, and orientation of the Al particles in the HDPE matrix were important factors in determining mechanical properties. The strength of the adhesive bond between two phases, the type of dispersion, and the amount of particle agglomeration also greatly affect mechanical properties. It is difficult to provide these effects in the samples since the homogeneity of the particle distribution is not uniform and the shape of the particles is not properly spherical.

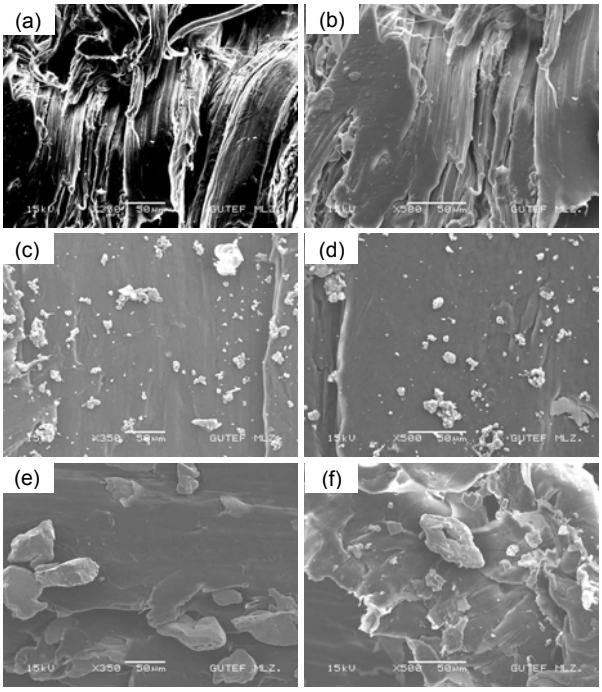

Fig. 9 Fracture surface of the samples
(a) and (b) HDPE with magnifications of 350X and 500X; (c) and (d) HDPE-Al containing 10% (v/v) Al with magnifications of 350X and 500X; (e) and (f) HDPE-Al containing 30% (v/v) Al with magnifications of 350X and 500X

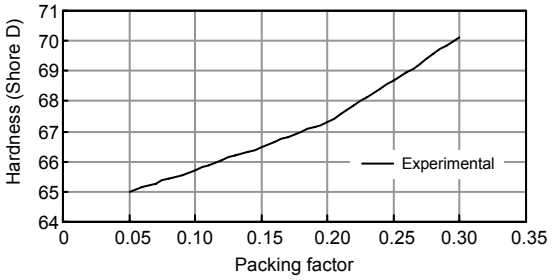

Fig. 10 Hardness of HDPE-Al composites

Nielsen (1974) developed a mathematical model which can predict tensile strength of polymer matrix composites reinforced with metal powders:

$$\sigma_c / \sigma_m = 1 - K_3 \varphi^{2/3}, \quad (7)$$

where σ_c and σ_m are the tensile strengths of the composite and the polymer matrix, respectively, K_3 is the constant that describes the quality of adhesion between the polymer matrix and the metal powders, and φ is the packing factor.

Comparing Nielsen (1974)'s model theoretical data with our experimental data, and calculating the coefficient K_3 from the Nielsen equation by regression analyses:

$$\sigma_c = \sigma_m (1 - 8.64\varphi^{2/3}), \quad (8)$$

and it was found K_3=8.64.

A decrease of elongation at break with an increase in the filler content is always observed. For description of this behaviour, the Nielsen model has been suggested as follows:

$$\varepsilon_{bc} = \varepsilon_{bm} (1 - \Phi_f^{K_1}), \quad (9)$$

where ε_{bc} and ε_{bm} are the elongations at break of the composite and the matrix polymer, K_1 is the constant that describes the quality of adhesion between the polymer matrix and the metal powders, Φ_f is the volume fraction of metal powder in the composite. For elongation at break, the coefficient K_1 was calculated from the Nielsen equation by regression analyses:

$$\varepsilon_{bc} = \varepsilon_{bm} (1 - \Phi_f^{0.25}), \quad (10)$$

and it was found K_1=0.25.

The ultimate tensile strength (UTS) and elongation at break of HDPE-Al composites were presented in Figs. 11 and 12. The Nielsen model is valid for particles of spherical shape assuming perfect adhesion between phases. Many types of filler do not fulfil these conditions. As shown in Fig. 4, the used metallic powders have very irregular shapes and consist of many sharp edges. These geometrical factors are expected to contribute significantly to a dramatic decrease of elongation at break. Conversely, the use of the Nielsen model is correct only if a deformation is homogeneous. In the case of polyethylene, a neck is created during tensile and therefore elongation at break is not homogeneous. The presence of defects in the front of the neck has a critical influence on the tensile behaviour of the composite.

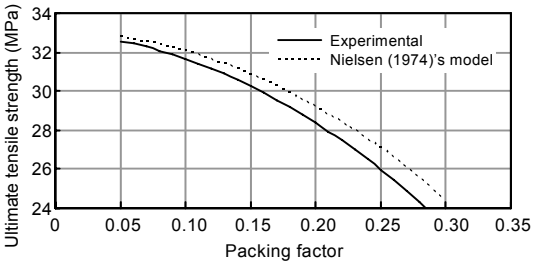

Fig. 11 Ultimate tensile strength of HDPE-Al composites

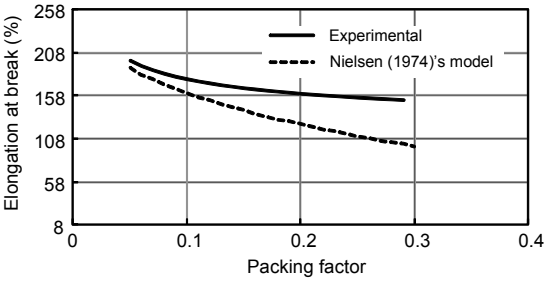

Fig. 12 Elongation at break of HDPE-Al composites

Experimental results concerning UTS and elongation were validated, by comparing them with the Nielsen model. As shown in Figs. 11 and 12, experimental values were higher than those obtained from the Nielsen mathematical model for UTS and elongation. This could be explained by the tendency of the agglomeration of powder particles, or by wetting and hence their poor encapsulation in the polymer matrix. The decline in the value of elongation at break (Fig. 12) with increasing addition of metal powder relative to that predicted by the mathematical model of Nielsen was due to lower adhesion between the phases. UTS and elongation at break decreased even though a small percent of Al particles were introduced into the polymeric matrix. Therefore, it is possible to state that adding Al particles into HDPE made the composite more brittle.

To describe the elastic modulus of the polymer matrix composite several mathematical models were found (Nielsen and Landel, 1994; Einstein, 2005), one of which is Einstein (2005)'s equation:

$$E_c = E_m(1-\Phi_f), \tag{11}$$

where E_c and E_m are the elastic moduli of the composite and the matrix polymer, respectively.

The second of these models is Nielsen and Landel (1994)'s equation, to describe the dependency of the elastic modulus versus powder content using the set of equations:

$$E_c = \frac{E_m(1+A\beta\Phi_f)}{(1-\beta\Psi_1\Phi_f)}, \tag{12}$$

$$\beta = \frac{(E_f/E_m-1)}{(E_f/E_m+A)}, \tag{13}$$

$$\psi_1 = 1+\frac{(1-\Phi_m)\Phi_f}{\Phi_m^2}, \tag{14}$$

$$A = \frac{7-5\nu}{8-10\nu}, \tag{15}$$

where E_f is the metallic powder elastic modulus, Φ_f is the volume percent of Al powder, β is the function of the elastic module of the composite, Φ_m is the volume fracture of matrix, ν is Poisson ratio of the matrix, and A is the function of Poisson ratio. The factor Ψ_1 can be determined by the maximum packing factor of composite.

Einstein (2005)'s mathematical model is valid at concentrations up to 30% volume metal powder incorporated into the polymer matrix and assumes a perfect adhesion between polymer and metal powder and a perfect dispersion of polymer particles in the metal powder matrix. As shown in Fig. 13, the Einstein model was almost validated by experimental data obtained. The experimentally values of modulus of elasticity were greater than those predicted by the Einstein model at 15% (v/v) Al. Theoretical values of elastic modulus according to the Nielsen model showed an increasing trend with increasing modulus of elasticity in the HDPE matrix with addition of Al powder. It appears that, for all concentrations considered, experimentally determined values are lower than those associated with the Nielsen model and the difference increases with increasing Al powder content (Fig. 13). It could be concluded that the Einstein model was more suitable than the Nielsen model for comparison of theoretical data with this experimental data.

Nielsen (1974) developed a mathematical model, which may provide electrical conductivity of polymer matrix composites reinforced with metal powders, expressed by

$$K_c = \frac{K_m(1+AB\Phi_f)}{(1-B\Psi_2\Phi_f)}, \tag{16}$$

$$B = \frac{K_f/K_m-1}{K_f/K_m+A}, \tag{17}$$

$$\psi_2 = \frac{1+\Phi_m(1-D_f)}{D_f^2}, \tag{18}$$

$$D_f = \frac{5}{\frac{75}{10+A_r}+A_r}, \tag{19}$$

where A_r is the function of the aspect ratio and orientation, B is a constant (B=1 for polymer systems), D_f is the maximum packing factor, Ψ_2 is determined by the maximum packing factor of composite, and K_c, K_m, and K_f are the conductivities of the composite, matrix, and filler, respectively. Nielsen (1974) used these equations to describe the electrical conductivity, thermal conductivity and the modulus of metal/polymer systems.

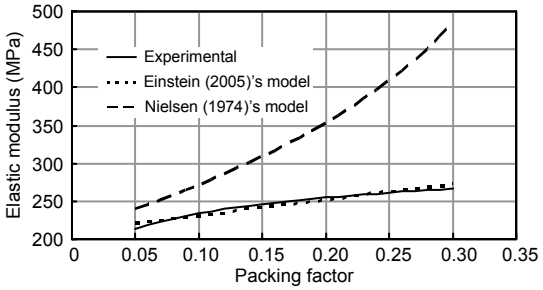

Fig. 13 Elastic modulus of HDPE-Al composites

Percolation is a change of the conductivity of a composite material taking place in a relatively narrow range of concentrations of dispersed conductor phase. It is caused by the formation of networks of conductive particles, at first fragmented and then continuing to significantly alter the electrical conductivity (heat). Increasing volume concentration of dispersed phase causes, in ideal conditions, an increase in particles per unit volume of composite material and therefore a decrease in distance between two neighbouring particles (dispersed phase). Increasing volume concentration of dispersed phase in the composite material causes these to reach a critical threshold called percolation threshold in which conductive particles are

attained by changing the character of insulating composite to conductor material composite.

When the reinforcing metallic powder had a random distribution into the composite matrix-identified by observation at SEM (Fig. 9), the polymer matrix composite had an increase in electrical conductivity (Fig. 14), because the percolation effect was formed at this critical volume fraction of the metal particles as a consequence of higher agglomeration of particles. The percolation effect is a well-known phenomenon observed in filler-matrix systems as the extreme change of certain physical properties within a rather narrow concentration range of heterogeneity (Kuo and Gupta, 1995; Gavarri *et al.*, 1999). The effect was explained as the formation of a conductive path through the sample in such a way that the conductive particles, which create the path, are in contact at a filler concentration corresponding to the percolation threshold.

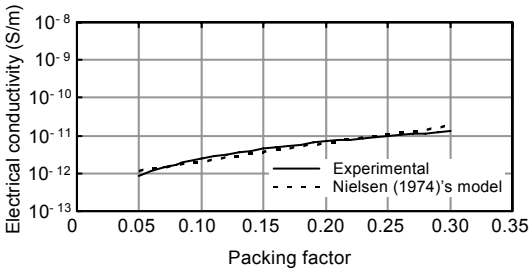

Fig. 14 Electrical conductivity of the HDPE-Al composites

Al particles with irregular shapes had long branches reaching out from the main body of the particle. Al powder can require anywhere from 5% to 30% loading to reach the percolation threshold. As shown in Fig. 14, experimental data were in good agreement with the theoretical values predicted by the Nielsen model.

Incorporation of the conductive Al powder as a reinforcing component in HDPE improved the thermal conductivity of the polymer matrix. The experimental results concerning thermal conductivity were validated by comparing them with those of Agari *et al.* (1990)'s model:

$$\log K_c = \log C_3 + \varphi C_2 \log K_f + (1-\varphi)\log(C_1 K_m), \quad (20)$$

where C_1 and C_2 are the coefficients.

Fig. 15 shows the determined thermal conductivity experimental data and prediction data obtained by the Agari model of HDPE-Al composites. The model coefficients C_1 (0.91), C_2 (0.18), and the equation constant C_3 (1.06) from Eq. (20), were obtained by regression analyses based on Al powder properties (type, filler dimension, and particle shape). Eq. (21) showed the Agari model adapted for Al powder used in this work as a reinforcing phase into the HDPE matrix:

$$K_c = 1.06 K_f^{0.18\varphi} 0.91 K_m^{1-\varphi}. \quad (21)$$

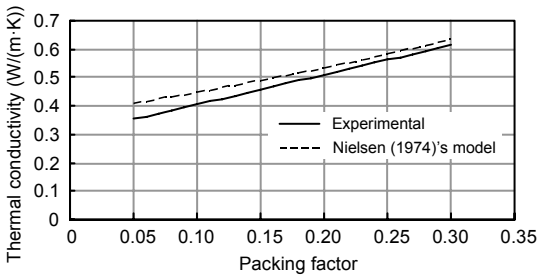

Fig. 15 Thermal conductivity of the composites as a function of Al content

As shown in Fig. 15, experimental values were validated by predicted values, and it can be seen that there was a clear increase in thermal conductivity of HDPE-Al composites with increasing Al content. This may be explained by the higher thermal conductivity of Al. The Al particles were located in the interlamellar spaces, in close contact with the lamellar surfaces. The high thermal conductivity of Al then caused these particles to quickly reach a higher temperature than the surrounding matrix (through the percolation pathways observed for high Al content composites). The consequence was the increase in thermal conductivity proportional to the reinforcing level of Al in the HDPE matrix.

4 Conclusions

In this paper, the mechanical and physical properties of HDPE-Al polymer composites were investigated and compared with general mathematical models.

In order to establish the suitable process parameters of injection moulding of composite, the main rheological parameters (viscosity, shear rate, and MFR) of HDPE-Al composites were studied. The values of MFR were measured for every rate of me-

tallic powder content between 5%–30%. Coefficient n was calculated as 0.7649.

As an original contribution, a new formula was generated by regression analyses for MFR according to density. It was found that MFR formula depends on the composite density, which agreed well with experimental data. This model has not been confirmed for the composite containing more than one type of reinforcing element.

The strength of the adhesive bond between two phases, the type of dispersion, and the amount of particle agglomeration also greatly affected the mechanical properties. It was difficult to provide these effects at all times since the homogeneity of the particle distribution was not uniform and the shape of the particles was not properly spherical.

The shape, distribution, and the volume fraction of metallic powder content in the HDPE matrix are important factors for controlling the mechanical properties of polymer matrix composite. With increasing reinforcing component, UTS and elongation at break decreased. This was due to the fact that the particle presence induced numerous discontinuities in the polymer matrix and, as a result, the composite ductility decreased. Elastic modulus obtained from experimental results was found to increase at higher Al powder contents in the HDPE matrix composites. UTS and elongation at break experimental data were compared with the Nielsen model and were found to agree well with mathematical model.

Elastic modulus experimental values were compared with the Nielsen and Einstein models, and it was concluded that the Einstein equation was more suitable for this experimental work.

Electrical and thermal conductivities of HDPE-Al composites depended on Al powder conductivity and polymer matrix conductivity. Electrical conducting paths and networks were formed in composites with increasing Al concentration. Electrical conductivity experimental data were compared with those of the Nielsen model, and it was concluded that all experimental data fit the Nielsen model. Thermal conductivity was compared with the Agari model, and it was found that the equation established was in a good agreement with the experimental data.

Incorporation of the conductive metal powder as a reinforcing component in polymers improved the electrical and thermal conductivities of the HDPE matrix. The electrical and thermal conductivities of composite materials obtained by mixing HDPE with sufficient contents of Al powder were superior to those of unfilled HDPE. It had been seen that thermal conductivity increased continuously up to 30% (v/v) Al. This was due to the fact that the percolation effect was formed at this critical volume fraction of the metal particles.

As a conclusion, the mathematical models were suitable to validate the experimental data, and the suitable coefficients and constant are obtained by regression analyses for the composites. It can be concluded that all the elaborated polymer matrix composites have good physical and mechanical properties and, as a result, can be used as multifunctional materials.

Acknowledgements

The author would like to express appreciations to the Technical University of Cluj-Napoca, Romania, for Erasmus Programme, and to the Mechanical and Material Education Department, Technical Education Faculty, Gazi University, Turkey, for providing the facility for this work.

References

Agari, Y., Ueda, A., Tanaka, M., Nagai, S., 1990. Thermal conductivity of a polymer filled with particles in the wide range from low to super-hight volume content. *Journal of Applied Polymer Science*, **40**(5-6):929-941. [doi:10.1002/app.1990.070400526]

ASTM C177-04, 2004. Standard Test Method for Steady-State Heat Flux Measurements and Thermal Transmission Properties by Means of the Guarded-Hot-Plate Apparatus. ASTM International, West Conshohocken, PA, USA.

ASTM D1238-10, 2010. Standard Test Method for Melt Flow Rates of Thermoplastics by Extrusion Plastometer. ASTM International, West Conshohocken, PA, USA.

ASTM D2240-05, 2010. Standard Test Method for Rubber Property—Durometer Hardness. ASTM International, West Conshohocken, PA, USA.

ASTM D257-07, 2007. Standard Test Methods for DC Resistance or Conductance of Insulating Materials. ASTM International, West Conshohocken, PA, USA.

ASTM D3835-08, 2008. Standard Test Method for Determination of Properties of Polymeric Materials by Means of a Capillary Rheometer. ASTM International, West Conshohocken, PA, USA.

ASTM D638-10, 2010. Standard Test Method for Tensile Properties of Plastics. ASTM International, West Conshohocken, PA, USA.

Bader, M.G., 2002. Selection of composite materials and manufacturing routes for cost-effective performance. *Composites Part A: Applied Science and Manufacturing*, **33**(7):913-934. [doi:10.1016/S1359-835X(02)00044-1]

Einstein, A., 2005. Einstein's Annalen Papers: The Complete Collection 1901–1922. *In*: Renn, J. (Ed.), Wiley-VCH Verlag GmbH, Germany (in German).

Gavarri, J.R., Tortet, L., Musso, J., 1999. Transport properties and percolation in two-phase composites. *Solid State Ionics*, **117**(1-2):75-85. [doi:10.1016/S0167-2738(98)00250-1]

Jang, J., Han, S., 1999. Mechanical properties of glass-fiber Mat/PMMA functionally gradient composites. *Composites Part A: Applied Science and Manufacturing*, **30**(9):1045-1053. [doi:10.1016/S1359-835X(99)00021-4]

Kovacs, J.Z., Velagala, B.S., Schulte, K., Bauhofer, W., 2007. Two percolation thresholds in carbon nanotube epoxy composites. *Composites Science and Technology*, **67**(5):922-928. [doi:10.1016/j.compscitech.2006.02.037]

Kuo, C.H., Gupta, P.K., 1995. Rigidity and conductivity percolation thresholds in particulate composites. *Acta Metallurgica et Materialia*, **43**(1):397-403. [doi:10.1016/0956-7151(95)90296-1]

Lux, F., 1993. Models proposed to explain the electrical conductivity of mixtures made of conductive and insulating materials. *Journal of Materials Science*, **28**(2):285-301. [doi:10.1007/BF00357799]

Nielsen, L.E., 1974. The thermal and electrical conductivity of two-phase systems. *Industrial and Engineering Chemistry Fundamentals*, **13**(1):17-20. [doi:10.1021/i160049a004]

Nielsen, L.E., Landel, R.F., 1994. Mechanical Properties of Polymers and Composites (2nd Ed.). Marcel Dekker, NY, USA.

Park, C.H., Saouab, A., Bréard, J., Han, W.S., Vautrin, A., Lee, W.I., 2009. An integrated optimisation for the weight, the structural performance and the cost of composite structures. *Composites Science and Technology*, **69**(7-8):1101-1107. [doi:10.1016/j.compscitech.2009.02.002]

Progelhof, R.C., Throne, J.L., Ruetsch, R.R., 1976. Methods for predicting the thermal conductivity of composite systems: a review. *Polymer Engineering and Science*, **16**(9):615-625. [doi:10.1002/pen.760160905]